

Whole-Heart Myofiber Tractography Derived From Conjoint Relaxation and Susceptibility Tensor Imaging

Russell Dibb^{1,2} and Chunlei Liu^{3,4}

¹Center for In Vivo Microscopy, Duke University Medical Center, Durham, North Carolina, United States, ²Biomedical Engineering, Duke University, Durham, NC, United States, ³Brain Imaging & Analysis Center, Duke University Medical Center, Durham, NC, United States, ⁴Radiology, Duke University Medical Center, Durham, NC, United States

Purpose: Susceptibility tensor imaging (STI) has been successfully applied as a preclinical imaging tool, particularly in magnetic resonance histology studies.¹ While STI can be used to probe tissue microstructure, it is limited by artifacts due to errors in phase processing, as well as noise. Relaxation tensor imaging (RTI) is another susceptibility-based MRI technique that has been used to probe tissue structure.^{2,3} We propose a strategy for improving the accuracy of STI through joint estimation of susceptibility and relaxation tensors in order to probe the microstructure and fiber architecture of magnetically anisotropic tissues, such as the myocardium,⁴ in 3D. Myofiber orientation and structure are important determinants of myocardial stress and strain⁵ and are altered by cardiac disease.⁶ Joint estimation of these two susceptibility-related tensors may potentially be used to assess the structure and function of both healthy and diseased hearts.

Methods: An adult, male C57BL/6 mouse was anesthetized with Nembutal and perfused via jugular vein at a rate of 8 ml/min by a peristaltic pump with 1) a 40 ml solution of 0.2% heparin in 0.9% saline to flush out the blood, 2) a 150 ml solution of 10% ProHance in 10% formalin to fix the tissue, and 3) 20 ml of 1.3% agarose gel. The blood and perfusion solutions were allowed to clear through the inferior vena cava and descending thoracic aorta. After the gel in the heart chambers solidified, the heart was excised and stored for three days in a solution of 0.5% ProHance in 10 mM phosphate-buffered saline. Magnitude and phase data were acquired at 9.4 T using a multiple-gradient-recalled echo (MGRE) sequence (array=512³, 8 echoes, res=30 μ m isotropic, TR = 50 ms, FA = 50°, TE₁/ΔTE/TE_n=3.0/5.5/41.5 ms) with the myocardium specimen positioned in $n=18$ different orientations with respect to the magnetic field. Diffusion tensor imaging (DTI) data were acquired with a 3D diffusion-weighted spin-echo sequence (array=400×300², res=30 μ m isotropic, TR = 50 ms, TE=15.4 ms); one scan with $b = 0$ s/mm², 12 diffusion-encoded scans with $b = 1,000$ s/mm² and diffusion time = 9.6 ms. The MGRE phase data underwent unwrapping and background phase removal using HARPERELLA.⁷ The susceptibility tensor data (\mathbf{X}) were reconstructed from the normalized image phase using STI Suite⁷ by effectively solving the minimization problem, $\min_{\mathbf{X}} \left(\sum_{i=1}^n \|p_i\|_2^2 \right)$, where $p_i = \mathbf{A}_i \mathbf{X}(\vec{k}) - \hat{\theta}_i(\vec{k})$. \vec{k} is the spatial frequency vector, and \mathbf{A}_i represents the k-space relationship that maps the susceptibility, $\mathbf{X}(\vec{k})$, to the normalized phase, $\hat{\theta}_i(\vec{k})$, for the i^{th} specimen orientation as described in [8]. R_2^* was calculated from a log-transformed linear fit of the MGRE magnitude images, and the relaxation tensor data were computed by fitting a second-order tensor to the apparent relaxation rate according to $\min_{\mathbf{R}} \left(\sum_{i=1}^n \|q_i\|_2^2 \right)$, where $q_i = \hat{\mathbf{H}}_i^T \mathbf{R} \hat{\mathbf{H}} - r_{2,i}$, $\hat{\mathbf{H}}_i$ is the field direction unit vector, and $r_{2,i}$ is the apparent relaxation rate. The major and minor eigenvectors of the susceptibility and relaxation tensors, respectively, are associated with the myofiber orientation. To take advantage of this mutual eigenvector information, conjoint relaxation and susceptibility tensor imaging (CRSTI) was implemented to simultaneously estimate these two tensors by solving the minimization problem described by $\min_{\mathbf{R}, \mathbf{X}} \left(\sum_{i=1}^n \|p_i\|_2^2 + \alpha \sum_{i=1}^n \|q_i\|_2^2 + \beta \left\| \mathbf{1} - \left| \hat{\mathbf{U}}_X^T \hat{\mathbf{U}}_R \right| \right\|_2^2 \right)$. Here, α and β are regularization parameters, and $\hat{\mathbf{U}}_X$ and $\hat{\mathbf{U}}_R$ represent the major susceptibility and minor relaxation eigenvectors, respectively. The DTI data were reconstructed using Diffusion Toolkit.⁹ Whole-heart tractography was then performed on the STI, CRSTI, and DTI data using TrackVis.⁹

Results: Fig. 1 shows the myofiber orientation maps produced by STI, CRSTI, and DTI. The STI data exhibit large myofiber orientation errors with respect to DTI. Much of this error is reduced in the CRSTI myofiber map, particularly in the left ventricle wall. The median myofiber orientation error was 53.1° for traditional STI, 33.5° for RTI, and 30.8° for CRSTI. Compared to traditional STI, CRSTI yields whole-heart tractography that more closely resembles DTI (Fig. 2).

Discussion and Conclusion: CRSTI is a useful step towards the robust estimation of tensor-valued susceptibility in the heart, though the technique could be improved through more accurate and sophisticated approaches to solving the joint-tensor minimization problem. STI and RTI suffer from artifacts due to imperfect background phase removal and bulk inhomogeneity, respectively. By combining STI and RTI data, CRSTI takes advantage of mutual tensor information in order to reduce myofiber orientation error and facilitates the application of susceptibility-based tractography to the heart for the first time. This requires no additional scan time since phase and relaxation data may be acquired simultaneously. The addition of eigenvector regularization to STI reconstruction will aid in examining animal models of myocardial disease *ex vivo* and provide additional tools for studying the source(s) of susceptibility contrast and anisotropy in the heart and other magnetically anisotropic tissues.

References: 1. Xie L, et al. Magn Reson Med 2014;10:1002/mrm.25219. 2. Wisniewski C, et al. Proc 22nd ISMRM 2014;893. 3. Lee J, et al. Neuroimage 2011;57:225-234. 4. Dibb R, et al. Proc 22nd ISMRM 2014;627. 5. Waldman LK, et al. Circ Res 1988;63:550-562. 6. Tezuka F. Tohoku J Exp Med 1975;117:289-297. 8. Li W, et al. NMR Biomed 2014;27:219-227. 8. Liu C. Magn Reson Med 2010;63:1471-1477. 9. Wang R, et al. Proc 15th ISMRM 2007;3720.

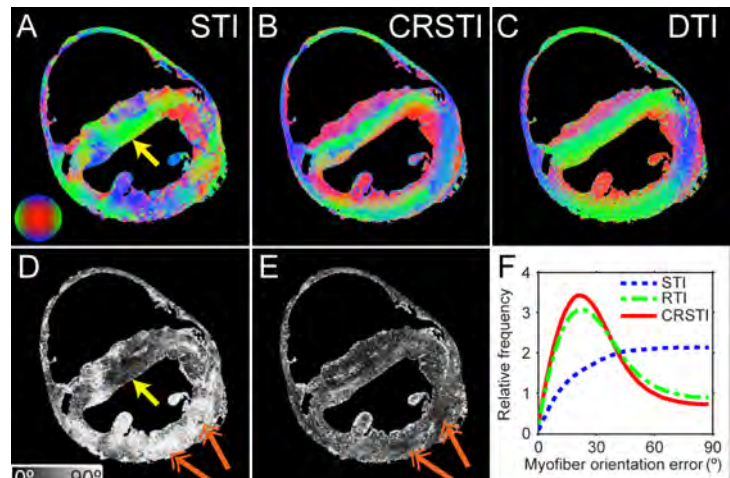


Fig. 1 Myofiber orientation maps for myocardium susceptibility tensor data reconstructed using STI (A) and CRSTI (B). The DTI orientation map (C) is the “gold standard” used to calculate myofiber orientation errors for the STI (D) and CRSTI (E). The distribution of the voxelwise error (F) shows that CRSTI yielded less error than both STI and RTI. Yellow arrows indicate an area of the septum where STI was most accurate, and orange arrows indicate areas of the LV wall where CRSTI most significantly reduced STI error.

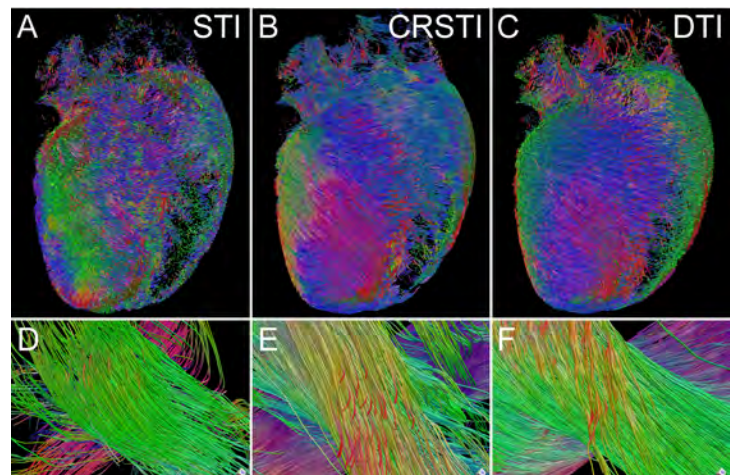


Fig. 2 Myofiber tractography derived from STI (A), CRSTI (B), and DTI (C) data. Traditional STI (D) was most successful in the septum, though myofiber tracking was further improved by CRSTI (E) to better resemble DTI (F).